J. Phys. B: Atom. Molec. Phys., Vol. 9, No. 10, 1976. Printed in Great Britain.

Experimental–theoretical comparisons of $1^1S \rightarrow 3^1P$ differential magnetic sublevel cross sections for electron–helium scattering at 80 and 100 eV†

Ara Chutjian
Jet Propulsion Laboratory, California Institute of Technology, Pasadena, California 91103, USA

Received 13 January 1976

Abstract. Experimental normalized absolute differential cross sections (DCS) for the excitation $1^1S \rightarrow 3^1P$ in helium are reported at incident electron energies of 80 and 100 eV, and at scattering angles between 7° and 135°. The measurements are combined with results of recent electron–photon coincidence studies, and absolute DCS for the excitation of the magnetic sublevels 3^1P_0 and $3^1P_{\pm 1}$ are obtained. These experimental sublevel cross sections, and their sum, are compared with results of recent calculations in the multichannel eikonal and distorted-wave polarized-orbital theories.

1. Introduction

In an earlier publication (Chutjian and Srivastava 1975, to be referred to as I), absolute differential magnetic sublevel cross sections were reported for the $1^1S \rightarrow 2^1P$ excitation in helium at electron energies of 60 and 80 eV. In the present paper these measurements are extended to the $1^1S \rightarrow 3^1P$ transition at energies of 80 and 100 eV. As in I, the present measurements of the differential cross section (DCS) at each energy are recombined with the recent electron–photon coincidence studies of Eminyan *et al* (1975) to give absolute differential magnetic sublevel cross sections over the range of scattering angles included in the latter measurements.

If one denotes the DCS of the $1^1S \rightarrow 3^1P$ transition as σ, then the present measurement gives the sum $\sigma_0 + \sigma_1$, where σ_0 and σ_1 are the $m = 0$ and twice the $m = 1$ sublevel cross sections, respectively, in the $1^1S \rightarrow 3^1P_{0,\pm 1}$ excitation. The measurements of Eminyan *et al* (1975) provide the scattering parameters χ (the magnitude of the phase difference of the $m = 0$ and $m = \pm 1$ excitations) and the cross section ratio $\lambda = \sigma_0/\sigma$. By combining λ and σ at each scattering angle θ and electron energy E_0, one obtains from experiment alone the absolute magnetic sublevel cross sections given by $\sigma_0 = \sigma\lambda$ and $\sigma_1 = \sigma(1 - \lambda)$. These experimental quantities may then be compared to the same quantities calculated by theory. Through such a comparison, one is able to make distinctions between theories which are not possible on the

† Work supported by the National Aeronautics and Space Administration under Contract NAS7-100 to the Jet Propulsion Laboratory. A preliminary report of this work was given at the 28th Gaseous Electronic Conference in Rolla, Missouri, USA (1976 *Bull. Am. Phys. Soc* **21** 158).

basis of σ alone (see I). Moreover, in the 3^1P case one expects channel couplings to become increasingly important since the states in the $n = 3$ manifold lie closer together in energy, and there are more of them; also the $n = 2$ manifold lies lower with much larger excitation cross sections. The 3^1P magnetic sublevel cross sections thus provide a further critical test of electron–atom scattering theories in the intermediate energy range. In the present work σ_0 and σ_1 are compared to the results of the multichannel eikonal theory (MET) (Flannery and McCann 1975) and the distorted-wave polarized-orbital theory (DWPO) (Scott and McDowell 1975, and private communication).

2. Experimental details

The apparatus and methods used in the measurements have been described earlier (see Chutjian 1974, and I). In the present work, the quantity measured was the ratio of peak heights or integrated areas of the *combined* $1^1S \rightarrow 3^1P$, $3^{1,3}D$ excitation relative to the elastic scattering. An energy-loss spectrum was obtained at each E_0 and θ in which the focusing was optimal for both the elastic and inelastic features. This procedure and details of the angle and energy-scale calibration are given in I. Multiplication of the inelastic-to-elastic ratio by the appropriate helium elastic scattering DCS (§2.1), correction for the finite angular resolution of the spectrometer (§2.2),

Table 1. Experimental inelastic/elastic ratios, and measured and calculated absolute DCS for the $1^1S \rightarrow 3^1P$ excitation at 80 and 100 eV. A superscript indicates the power of 10 by which the entry should be multiplied. Extrapolated values are shown by parentheses.

			$3^1P(cm^2\ sr^{-1}) \times 10^{19}$					
	3^1P/elastic		80 eV			100 eV		
	80 eV (this work)	100 eV (this work)	Exp (this work)	Calc		Exp (this work)	Calc	
θ (deg)				MET[a]	DWPO[b]		MET[a]	DWPO[b]
0	—	—	(16^{+1})	20^{+1}	22^{+1}	(24^{+1})	26^{+1}	31^{+1}
5	$(1{\cdot}7^{-1})$	$(2{\cdot}9^{-1})$	(12^{+1})	18^{+1}	16^{+1}	(19^{+1})	23^{+1}	20^{+1}
7	$1{\cdot}4^{-1}$	$2{\cdot}5^{-1}$	92	16^{+1}	—	14^{+1}	18^{+1}	—
10	$1{\cdot}1^{-1}$	$1{\cdot}7^{-1}$	62	10^{+1}	84	82	96	86
15	$6{\cdot}8^{-2}$	$9{\cdot}4^{-2}$	28	36	39	33	28	34
20	$3{\cdot}5^{-2}$	$4{\cdot}8^{-2}$	11	11	17	12	8·6	13
25	$2{\cdot}0^{-2}$	$2{\cdot}1^{-2}$	4·7	4·4	7·5	4·0	2·9	5·0
30	$1{\cdot}2^{-2}$	$1{\cdot}0^{-2}$	2·4	1·7	3·1	1·5	1·0	1·9
40	$6{\cdot}6^{-3}$	$6{\cdot}0^{-3}$	$9{\cdot}0^{-1}$	$3{\cdot}5^{-1}$	$5{\cdot}4^{-1}$	$4{\cdot}5^{-1}$	$2{\cdot}1^{-1}$	$2{\cdot}8^{-1}$
50	$6{\cdot}4^{-3}$	—	$5{\cdot}6^{-1}$	$1{\cdot}2^{-1}$	$1{\cdot}3^{-1}$	—	$7{\cdot}5^{-2}$	$8{\cdot}0^{-2}$
60	$5{\cdot}9^{-3}$	$5{\cdot}0^{-3}$	$3{\cdot}8^{-1}$	$5{\cdot}6^{-2}$	$7{\cdot}3^{-2}$	$1{\cdot}2^{-1}$	$4{\cdot}2^{-2}$	$5{\cdot}0^{-2}$
90	$5{\cdot}4^{-3}$	$3{\cdot}7^{-3}$	$1{\cdot}3^{-1}$	$2{\cdot}7^{-2}$	$3{\cdot}7^{-2}$	$4{\cdot}1^{-2}$	$1{\cdot}2^{-2}$	$2{\cdot}4^{-2}$
110	$4{\cdot}2^{-3}$	$3{\cdot}7^{-3}$	$8{\cdot}1^{-2}$	$1{\cdot}4^{-2}$	$2{\cdot}3^{-2}$	$3{\cdot}2^{-2}$	$6{\cdot}8^{-3}$	$1{\cdot}5^{-2}$
135	$4{\cdot}4^{-3}$	$4{\cdot}3^{-3}$	$7{\cdot}1^{-2}$	$8{\cdot}5^{-3}$	$1{\cdot}4^{-2}$	$3{\cdot}3^{-2}$	$4{\cdot}2^{-3}$	$9{\cdot}3^{-3}$
150			$(6{\cdot}3^{-2})$	$6{\cdot}2^{-3}$	$1{\cdot}1^{-2}$	$(2{\cdot}8^{-2})$	$3{\cdot}4^{-3}$	$7{\cdot}5^{-3}$
160			$(6{\cdot}1^{-2})$	$5{\cdot}7^{-3}$	$9{\cdot}9^{-3}$	$(2{\cdot}7^{-2})$	$3{\cdot}3^{-3}$	$6{\cdot}8^{-3}$
180			$(5{\cdot}9^{-2})$	$5{\cdot}6^{-3}$	$9{\cdot}4^{-3}$	$(2{\cdot}7^{-2})$	$3{\cdot}3^{-3}$	$6{\cdot}3^{-3}$

[a] Calculated in the multichannel eikonal theory (Flannery and McCann 1975).
[b] Calculated in the distorted-wave polarized-orbital theory (Scott and McDowell 1975, and private communication).

and subtraction of the $3^{1,3}D$ state contributions (§2.3) then gave the absolute $1^1S \rightarrow 3^1P$ DCS.

2.1. Choice of the helium elastic scattering DCS

The intensity ratio, denoted as 3^1P, $3^{1,3}D$/elastic, when multiplied by the elastic scattering DCS gives the absolute DCS for the combined 3^1P, $3^{1,3}D$ excitation. Our choice of the helium elastic DCS at 80 eV was the same as in I. At 100 eV an analogous procedure to that in I was followed. The elastic DCS in the angular range $20° \leqslant \theta \leqslant 90°$ was taken from the measurements of McConkey and Preston (1975). At higher angles the measured DCS were lower than the calculated values of LaBahn and Callaway (1970). Our choice of DCS in the range $90° < \theta \leqslant 135°$ was to draw a smooth curve through the measured DCS (McConkey and Preston 1975), using the shape of the calculated DCS as a guide. The resultant DCS at 135°, for example, was 57% of the calculated value. At lower angles the measured absolute point of Chamberlain *et al* (1970) at 5° was used as a reference. The DCS in the angular range $0° \leqslant \theta < 20°$ was taken from a smooth curve passing through the 5° value and joining onto the experimental value at 20°. The resultant DCS was indistinguishable from the renormalized absolute measurements of Vriens *et al* (1968) and at 5° lay 11% above the calculated value of LaBahn and Callaway (1970).

Comparison is possible with the recent absolute elastic DCS measurements of Kurepa and Vušković (1975). These measurements are factors of 1·4–2·7 larger than the results of McConkey and Preston (1975) and the renormalized results of Vriens *et al* (1968) in the angular range $5° \leqslant \theta \leqslant 90°$. Regardless of this fact, the use of the Kurepa and Vušković elastic DCS appears to give integral 3^1P (and 2^1P, see I) cross sections about a factor of 1·4 larger than several theories and several independent measurements of the optical-excitation function (see table 1). We have therefore used both the McConkey and Preston and the extrapolated–interpolated DCS. As in I, we also report inelastic/elastic ratios so future improvements over these elastic DCS can be used to update the present inelastic DCS.

2.2. Effects of finite spectrometer angular resolution

Because the $1^1S \rightarrow 3^1P$ DCS at large E_0 is a strongly forward-peaked function of θ (see figure 1) the question arises as to the effect of the finite spectrometer angular resolution on the measured DCS. How much 'smearing' in angle is present in the DCS? If we denote $\sigma(\theta)$ and $\sigma^m(\theta)$ as the true and measured DCS respectively, then the effect of the slit may be expressed as the convolution

$$\sigma^m(\theta) = \int_{-\pi}^{\pi} \sigma(\theta - \theta')g(\theta')\,d\theta' \tag{1}$$

where $g(\theta)$ is the slit response function. Physically, one would expect the main effects of the slit broadening to be a lowering of the small-angle DCS and raising of the large-angle DCS. There will also be a small intermediate angular region, where the DCS has its inflection point, in which the DCS will be unaffected by the broadening. This may easily be seen by approximating $\sigma(\theta)$ near its inflection point by the linear function

$$\sigma(\theta - \theta') = a_0 + a_1(\theta - \theta').$$

Under the assumptions that $g(\theta)$ is (i) normalized to unity, (ii) a symmetric function of θ and (iii) has a width smaller than the linear region of $\sigma(\theta)$, one finds that

$$\sigma^{m}(\theta) = \int_{-\pi}^{\pi} [a_0 + a_1(\theta - \theta')]g(\theta')\,d\theta' = a_0 + a_1\theta = \sigma(\theta)$$

or that $\sigma(\theta)$ is not affected by the slit function in its linear region.

The form of $g(\theta)$ is difficult to obtain, but some reasonable estimates can be made from the present scattering geometry. We take the shape of $g(\theta)$ in equation (1) to be triangular and its base width to be the maximum angle ($\pm 2°$) subtended by the analyser at the scattering centre. The deconvolution according to equation (1) was carried out graphically. It was found that at both E_0 values the cross section $\sigma(\theta)$ was approximately 1% higher than $\sigma^{m}(\theta)$ in the range $0° \leqslant \theta \leqslant 8°$, 1–2% lower than $\sigma^{m}(\theta)$ in the range $15° \leqslant \theta \leqslant 40°$ and was equal to $\sigma^{m}(\theta)$ elsewhere. These systematic corrections were applied to the combined $1^1S \rightarrow 3^1P$, $3^{1,3}D$ excitation. For comparison, similar or only slightly larger corrections were found using a rectangular slit function of 4° base width.

2.3. Correction for the presence of the $3^{1,3}D$ excitations

Since the $1^1S \rightarrow 3^1D$ and $1^1S \rightarrow 3^3D$ transitions lay only 0·013 and 0·014 eV respectively from the 3^1P excitation, they could not be resolved in the energy-loss spectra recorded at resolutions varying from 0·038–0·055 eV (FWHM). To eliminate the contribution of the $^{1,3}D$ states several procedures were followed. Firstly, the measurements were carried out at relatively high incident electron energies so that the maximum

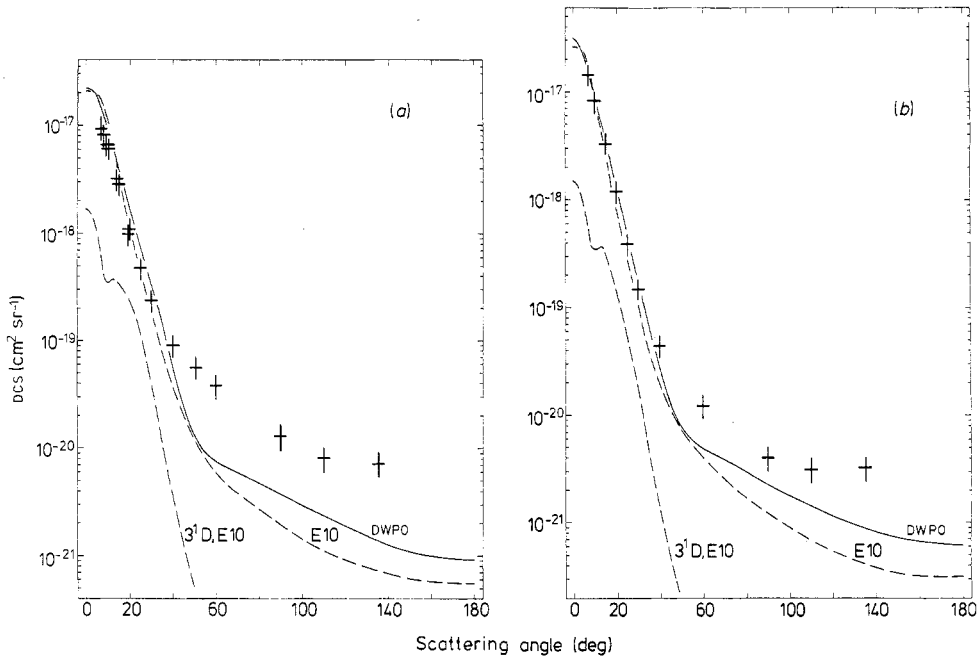

Figure 1. Experimental absolute differential cross sections (+) for the $1^1S \rightarrow 3^1P$ transition at an incident electron energy of (*a*) 80 eV and (*b*) 100 eV. Theoretical results are from Flannery and McCann (1975) (E10) and Scott and McDowell (1975, and private communication) (DWPO).

contributions of the ^1D and ^3D integral cross sections to the ^1P integral cross section were 9% and 1%, respectively (Moustafa Moussa *et al* 1969). The effect of the ^3D excitation was hereafter neglected (but see below). Secondly, the remaining 9% contribution of the ^1D state at 80 eV (6% at 100 eV) was subtracted from the slit-corrected 3^1P, $3^{1,3}D$ DCS by using the *shape* of the 3^1D DCS as calculated in the MET (Flannery and McCann 1975), renormalizing that shape to the experimental 3^1D integral cross section as measured by Moustafa Moussa *et al* (1969). This was deemed a reliable procedure at low angles since the 3^1D excitation is forward peaked, and the eikonal theory reliably accounts for the shape of the forward scattering. The renormalized 3^1D DCS are shown in figure 1. At higher angles (75–180°) it was found from previous calculations (see figures 7 and 8 of Chutjian and Thomas 1975) that the ratio $\sigma(^1D)/\sigma(^1P)$ fell rapidly by factors of two or more between 29·2 and 39·7 eV, to a value of about 0·1 at 136° and 39·7 eV. Assuming this trend to continue to 80 and 100 eV, one finds the contribution of the ^1D state at high angles to be negligible in the present measurements. By an analogous argument, one also expects the ^3D excitation to be negligible at high angles. Thus, both the low-angle (after correction) and high-angle portions of the ^1P DCS should be free of the $^{1,3}D$ state transitions.

3. Results

The ratio 3^1P/elastic and the $1^1S \rightarrow 3^1P$ DCS are listed in table 1 and shown in figure 1 with the results of calculations in the MET and DWPO theories. The experimental errors, given as one standard deviation of the mean, associated with the intensity ratios and the DCS are summarized in table 2 for the different corrections discussed in §2.

An important cross-check on the present DCS measurements (and therefore on σ_0 and σ_1) is the agreement between the integral cross sections derived from the present DCS and independent optical-excitation-function measurements. This agreement among the different experiments as well as calculations is shown in table 3. As noted in I, the integral cross sections for the strongly forward-peaked 2^1P and 3^1P

Table 2. Estimates of errors associated with the intensity ratios and DCS of table 1 and figures 1–2, for the angular ranges shown.

	Estimate of error (%)	
Source of error	0–59°	60–135°
Random error in ratio 3^1P/elastic	18	22
Angular deconvolution	2	0
Correction for $1^1S \rightarrow 3^1D$ excitation	3	1
Neglect of $1^1S \rightarrow 3^3D$ excitation	+0	+0
	−1	−1
Total RMS error in ratio 3^1P/elastic	18	22
Helium elastic DCS[a]	12	12
Total RMS error in the DCS	22%	25%

[a] From McConkey and Preston (1975). This error does not include any systematic error in the present extrapolation of the elastic DCS from 90° to 135°.

Table 3. Measured and calculated integral 3^1P cross sections, Q, at E_0 of 80 and 100 eV.

	$Q(cm^2) \times 10^{18}$			
	Experimental		Calculated	
Reference	80 eV	100 eV	80 eV	100 eV
This work	2·2 ± 0·5	2·8 ± 0·6		
Moustafa Moussa *et al* (1969)	2·47 ± 0·18	2·60 ± 0·19		
de Jongh and Van Eck (1971)	2·25	2·60		
Donaldson *et al* (1972)	2·92 ± 0·28	2·96 ± 0·29		
Flannery and McCann (1975) (E10)			2·86	2·79
Scott and McDowell (1975, and private communication) (DWPO)			2·92	2·89

DCS arise mainly from the first 40° or so of scattering. The agreement in table 3 thus confirms the small-angle scattering, which is also the region of the available λ values.

Using the DCS values in table 1 and the appropriate values of λ (table 2, Eminyan *et al* 1975) we obtain experimental values of σ_0 and σ_1. These quantities are plotted in figure 2 and compared to the two theoretical calculations.

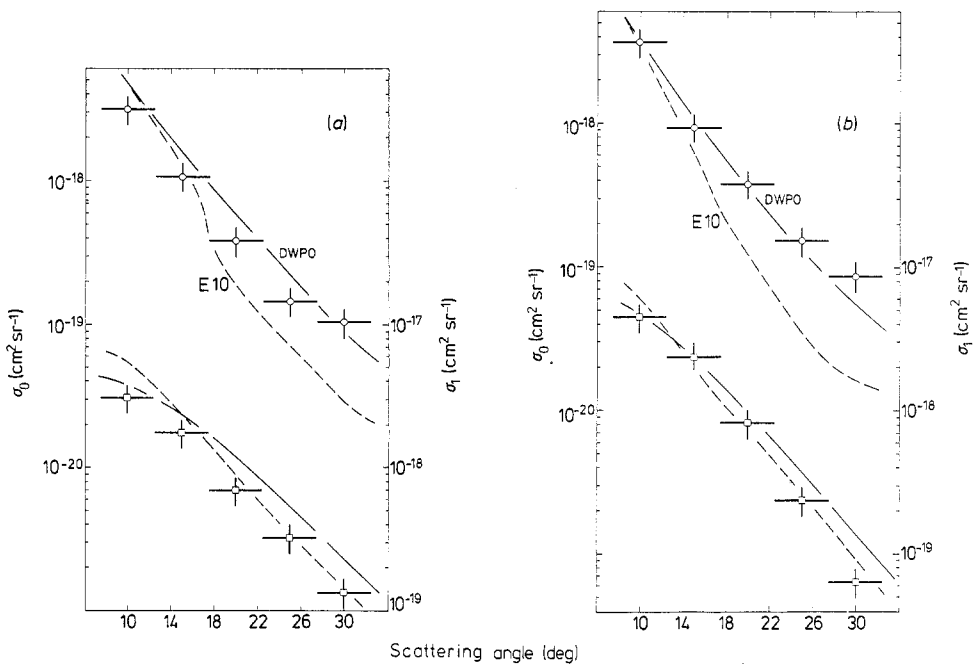

Figure 2. Experimental magnetic sublevel cross sections (+) for the $1^1S \rightarrow 3^1P$ transition at an incident electron energy of (*a*) 80 eV and (*b*) 100 eV. The quantity σ_0 (○) is the $1^1S \rightarrow 3^1P_0$ cross section, while σ_1 (□) is twice that of the $1^1S \rightarrow 3^1P_1$ excitation. Theoretical results are from Flannery and McCann (1975) (E10) and Scott and McDowell (1975, and private communication) (DWPO).

4. Discussion

As may be seen in figure 1, there is generally good agreement in the DCS between theory and experiment for θ in the range $7° \leqslant \theta \leqslant 40°$. At 80 eV both theories tend to lie slightly above the upper error limits of the present measurements in this angular range, while the agreement at 100 eV is excellent. These trends are also evident in the integral cross section values in table 3.

The disagreement at higher angles in the case of the MET is consistent with the fact that this theory neglects exchange effects, and is essentially a forward-scattering theory. The high-angle disagreement in the case of the DWPO theory may arise from neglect in the exchange scattering of higher-order effects, such as exchange polarization (M R C McDowell, private communication). As noted in §2.3 it is unlikely that the present measurements may be high at large angles due to any ^{1,3}D state contributions. Nor could a large value of the ^{1}P DCS arise from the use of a helium elastic DCS which was *itself* too large, since the extrapolated values used in the present work lie at the lower range of available measurements (for a summary see table 1 of Kurepa and Vušković 1975).

In the sublevel cross sections of figure 2 one finds good agreement of the DWPO values with the experimental σ_0 and σ_1, especially at 100 eV. In the case of the MET σ_1 is an excellent agreement with experiment, while σ_0 rapidly falls below experiment for $\theta > 15°$. This result is in agreement with the comparison on the basis of λ alone (see figure 9 of Flannery and McCann 1975) where the calculated λ was seen to drop below experiment for $\theta > 15°$, due to the too small calculated value of σ_0 (figure 2). Moreover, the trend in the MET cross sections is different than that in the 2^1P case. There, σ_0 was in good agreement with experiment, while σ_1 was too large (see figure 4 of I).

5. Conclusion

One thus sees that, while the DCS calculations alone (figure 1) appear to give comparable agreements with experiment, a more critical comparison based on the magnetic sublevel DCS (figure 2) shows significant differences in the two theoretical approximations. Such distinctions were also possible in the 2^1P case (see I).

Acknowledgments

We thank Dr S Trajmar for his encouragement of this work. We are also grateful to Professor M R Flannery and Dr K J McCann, and Professor M R C McDowell and Dr T Scott for their sublevel cross sections calculated in the multichannel eikonal and distorted-wave polarized-orbital theories, respectively. We acknowledge a helpful discussion with Dr G Joyez.

References

Chamberlain G E, Mielczarek S R and Kuyatt C E 1970 *Phys. Rev.* A **2** 1905–22
Chutjian A 1974 *J. Chem. Phys.* **61** 4279–84
Chutjian A and Srivastava S K 1975 *J. Phys. B: Atom. Molec. Phys.* **8** 2360–8

Chutjian A and Thomas L D 1975 *Phys. Rev.* A **11** 1583–95
Donaldson F G, Hender M A and McConkey J W 1972 *J. Phys. B: Atom. Molec. Phys.* **5** 1192–210
Eminyan M, MacAdam K B, Slevin J, Standage M C and Kleinpoppen H 1975 *J. Phys. B: Atom. Molec. Phys.* **8** 2058–66
Flannery M R and McCann K J 1975 *J. Phys. B: Atom. Molec. Phys.* **8** 1716–33
de Jongh J P and van Eck J 1971 *Proc. 7th Int. Conf. on Physics of Electronic and Atomic Collisions* (Amsterdam: North-Holland) Invited Papers pp 701–3
Kurepa M V and Vušković L 1975 *J. Phys. B: Atom. Molec. Phys.* **8** 2067–78
LaBahn R W and Callaway J 1970 *Phys. Rev.* A **2** 366–9
McConkey J W and Preston J A 1975 *J. Phys. B: Atom. Molec. Phys.* **8** 63–74
Moustafa Moussa H R, de Heer F J and Schutten J 1969 *Physica* **40** 517–49
Scott T and McDowell M R C 1975 *J. Phys. B: Atom. Molec. Phys.* **8** 1851–65
Vriens L, Kuyatt C E and Mielczarek S R 1968 *Phys. Rev.* **170** 163–9